THE INFLUENCE OF CURRENT DENSITY OF DEPOSITION ON PROPERTIES OF Zn–Ni COATINGS

K. WYKPIS, M. POPCZYK, J. NIEDBAŁA, A. BUDNIOK, E. ŁĄGIEWKA

University of Silesia, Institute of Materials Science, Katowice

Zn–Ni coatings were deposited under galvanostatic conditions at current density in the range of 20 to 60 mA·cm^{-2}. The influence of current density of deposition on the surface morphology, chemical and phase composition and corrosion resistance was investigated. Structural investigations were performed by the X-ray diffraction (XRD) method. The surface morphology and chemical composition of deposited coatings were studied using a scanning electron microscope JEOL JSM-6480. Studies of general electrochemical corrosion resistance were carried out in the 5% NaCl, using potentiodynamic and electrochemical impedance spectroscopy (EIS) methods. Local corrosion resistance was determined by Scanning Kelvin Probe (SKP) method. On the ground of the research, the possibility of deposition of Zn–Ni coatings containing 14…18 at.% Ni was shown. It was stated, that surface morphology, chemical and phase composition of these coatings to a small extent, depend on the current density of deposition. However, current density of deposition determines the quantity of zinc which is co-deposited with nickel and is bounded in the form of an intermetallic compound or a solid solution. Small differences in chemical composition and the uneven distribution of the Zn(Ni) and Ni$_2$Zn$_{11}$ phases on coatings surface may cause differences in the local Kelvin potential. As a result, the Zn–Ni coatings exhibit corrosion resistance that varies depending on the deposition current density. The optimal values of current density for the sake of corrosion resistance are found to be $j = 30$ and 40 mA·cm^{-2}.

Keywords: *electrodeposition, Zn–Ni coatings, corrosion resistance, SKP method.*

The interest in zinc and their alloys [1–4] results from the good corrosive resistance of these materials and search of a suitable alternative to toxic cadmium coatings.

It was proved, that corrosion resistance of Zn–Ni coatings depends on their chemical compositions, morphology of surface and structures [1, 5–8]. These properties are formed depending on the electrodeposition conditions [6, 8].

Studies of Zn–Ni deposition in electrolytes containing ammonia ions have shown that normal or anomalous codeposition takes place depending on the value of potential or cathodic current. As a result Zn–Ni coatings may contain from $\geq$ 95 wt.% to 15 wt.% Ni [9].

Electrolytic Zn–Ni alloys are characterized by the occurrence of a wider range of different phases. It was stated that nickel is dominant in a layer adjacent to the substrate, independently on a kind of the substrate. Next, zinc in the nickel solid solution (α-phase) is created, depending on the deposition current density [8]. Unlike an equilibrium metallurgical alloy, α- and β-phases are not formed in electrolytic Zn–Ni alloy. Using the potentiodynamic stripping method, potential values of current peaks were attributed to the values of selective dissolution of particular phases [10]. In this way, the γ-phase i.e. Ni$_5$Zn$_{21}$ and η-phase being 1% nickel in zinc solid solution, are formed. On the basis of electrochemical investigations it was found that the γ-phase is very chemically active by the selective dissolution of zinc. The high corrosion resistance and good mechanical properties of Zn–Ni layers are connected with the presence of the γ-phase i.e. Ni$_5$Zn$_{21}$.

The aim of the present work was to obtain of electrolytic Zn–Ni coatings and to determine of an influence of deposition current density on their chemical compositions, structure and corrosion resistance.

Experimental. Electrolytic Zn–Ni coating was obtained from the ammonia bath of composition (g·dm^{-3}): NiSO$_4$·7H$_2$O – 50; ZnSO$_4$·7H$_2$O – 100; Na$_2$SO$_4$ – 75; (NH4)$_2$SO$_4$ – 38; NH$_4$OH – 250 cm^3·dm^{-3}. The temperature of the bath was 298 K; pH was kept in the range of 9.6 to 10.4. The process of electrodeposition was carried out in the galvanostatic conditions at current density in the range of 20 to 60 mA·cm^{-2}.

The Zn–Ni coating was deposited on austenitic steel (OH18N9). The preparation of substrate surface consisted of the following steps: cleaning with a detergent solution, chemical treatment with HCl solution (1:1), rinsing in distilled water and degreasing.

Prior to deposition, the steel substrate was activated in HCl solution, using cathode current density $j = 5$ mA·cm^{-2}, for 2 min. The nickel underlayers, obtained from the bath containing 350 g·dm^{-3} NiCl$_2$·6H$_2$O and 111 cm^3·dm^{-3} HCl, were deposited before obtaining of the Zn–Ni coatings in order to assure adhesion of the Zn–Ni coating to the substrate.

The surface morphology and surface chemical composition of deposited coatings were studied using a scanning electron microscope (JEOL JSM-6480) with EDS attachment.

The XRD patterns were measured using the Philips X'Pert PW 3040/60 X-ray diffractometer with copper radiation ($\lambda_{K_\alpha} = 1.54056$ Å). A graphite monochromator was used to select the K_α radiation.

The electrochemical corrosion resistance of the prepared coatings was investigated in a three-electrode cell using the potentiodynamic and electrochemical impedance spectroscopy (EIS) methods. These measurements were carried out in 5% NaCl solution, at a temperature of 293 K using AUTOLAB® electrochemical system. The auxiliary electrode was a platinum mesh and the reference electrode was the saturated calomel electrode (SCE). The values of corrosion potential, corrosion current and polarization resistance were determined by the Stern method. The electrochemical impedance measurements were performed at the corrosion potential. In these measurements the amplitude of the ac signal 0.005 V. A frequency range from 10 kHz to 0.1 Hz was covered with ten points per decade.

The SKP measurements were made using a Scanning Electrochemical Workstation Model 370 (Princeton Applied Research AMETEK). The SKP scans were made of 300 μm × 300 μm area surface. The vibrating amplitudes of the scanning probe were adjusted to 30 μm. The Kelvin probe was placed above the surface of the Zn–Ni coatings at a height of about 300 μm. The topography of Zn–Ni coatings surface was characterized using Kelvin probe.

The corrosion behaviour of the Zn–Ni coatings was also examined using accelerated corrosion test in a salt chamber (HK 400, KOHLER) according to PN-EN ISO 9227. These coatings were subject to salt spray (5% NaCl) exposure at 308 K for 96 h.

Results and discussion. All obtained Zn–Ni coatings have a grey and smooth surface. These coatings show good adhesion to the substrate and lack of cracks. Only on the surface of the coating deposited at $j = 60$ mA·cm^{-2} small cracks are observed (Fig. 1).

The results of surface chemical composition analysis show, that the chemical composition of coatings depends to a small degree on the deposition current density and is in the range from 14.2±0.4 to 18.0±0.4 at.% Ni. The surface chemical composition initially decreases and then increases with an increase of deposition current density. The coating deposited at $j = 30$ mA·cm^{-2} is characterized by the least of the nickel contents e.g. 14.2 at.%.

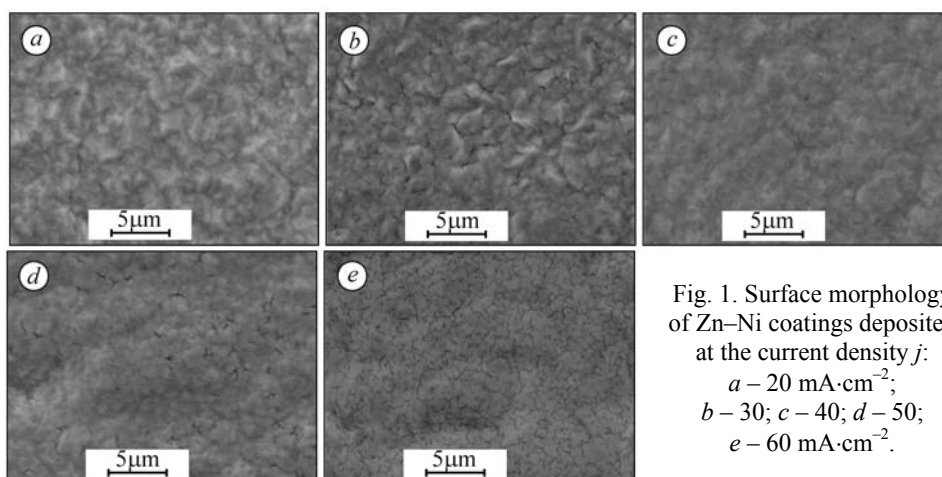Fig. 1. Surface morphology of Zn–Ni coatings deposited at the current density j: a – 20 mA·cm^{-2}; b – 30; c – 40; d – 50; e – 60 mA·cm^{-2}.

The X-ray phase analysis showed the differences in phase composition of the Zn–Ni coatings depending on the deposition current density (Fig. 2). The presence of reflexes coming from Zn phase shows only the XRD pattern of Zn–Ni coating deposited at j = 20 mA·cm^{-2}. All X-ray diffraction patterns show the presence of reflexes corresponding to the Zn(Ni) solid solution and Ni$_2$Zn$_{11}$ intermetallic phases. These phases are the result of co-deposition of zinc and nickel ions. The zinc content in nickel in the case of the Ni(Zn) solid solution, determined on the basis of the Vegard law, increases with an increase in deposition current density from about 23 to 30%. Thus, the current density influences the amount of zinc connected with nickel in the solid solution or the intermetallic compound. The differences in the phase composition and a non-uniform distribution of the Ni(Zn) and Ni$_2$Zn$_{11}$ phases on the surface of obtained coatings, may cause the differences in the coatings corrosion resistance.
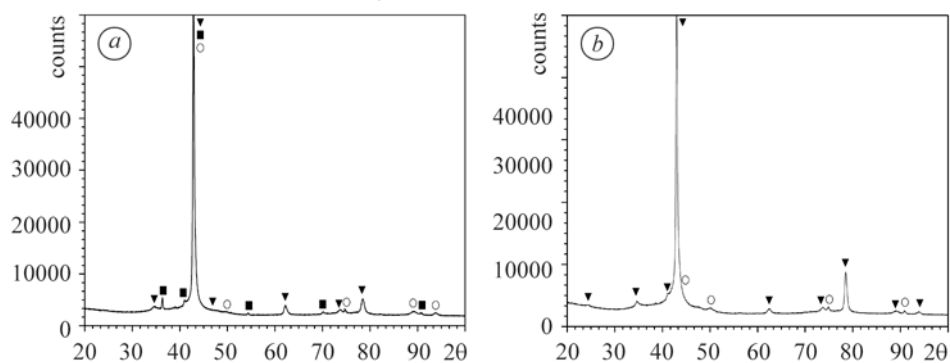

Fig. 2. X-ray diffraction pattern of Zn–Ni coating deposited at current density j: a – 20 mA·cm^{-2}; b – 50 mA·cm^{-2}. ■ – Zn; ▼ – Ni$_2$Zn$_{11}$; ○ – Ni(Zn).

Table 1. Corrosion parameters of Zn–Ni coatings determined by the potentiodynamic method depending on the current density of deposition j

j, mA·cm^{-2}	E_{cor}, V	j_{cor}, µA·cm^{-2}	R_p, kΩ·cm^2
20	−0.791	0.90	6.81
30	−0.755	0.14	37.41
40	−0.783	0.22	16.87
50	−0.807	0.81	8.45
60	−0.802	0.41	8.84

Open circuit potentials of the coatings were determined for 20 h. A range of ±0.050 V was chosen from the determined value and a potentiodynamic curve was recorded with a rate of v = 0.060 V·min^{-1}. On the ground of the obtained dependences $j = f\,(E)$, the values of corrosion parameters were determined. It was found that for the Zn–Ni coating obtained at j = 30 mA·cm^{-2},

the value of corrosion current is lower and the value of polarization resistance is higher compared with the other Zn–Ni coatings (Table 1). It is suggested, that the Zn–Ni coating obtained at $j = 30$ mA·cm^{-2} is more corrosion resistant in 5% NaCl solution than other Zn–Ni coatings.

Results of EIS investigations are submitted in the form of Nyquist and Bode diagrams ($Z'' = f(Z')$, $\log |Z| = f(\log \omega)$ and $\Phi = f(\log \omega)$) (Fig. 3–5).
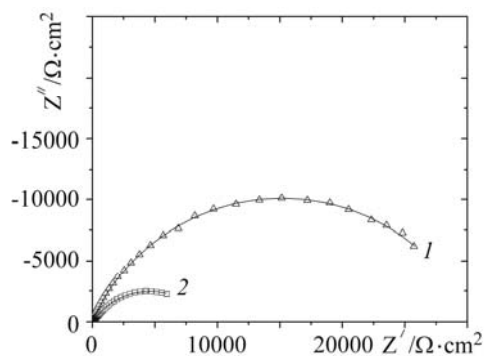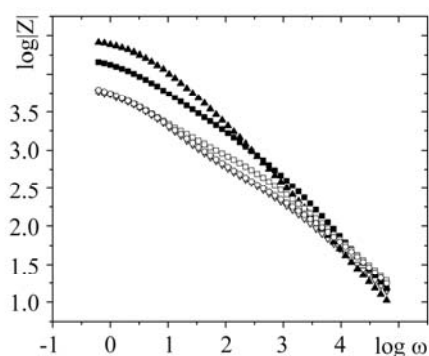

Fig. 3.   Fig. 4.

Fig. 3. Dependences of $Z'' = f(Z')$ for the Zn–Ni coatings obtained at the current densities: $j = 30$ mA·cm^{-2} (*1*) and 50 mA·cm^{-2} (*2*) ($\triangle$, $\square$ – experimental points; —— – approximation line).

Fig. 4. Dependences of $\log |Z| = f(\log \omega)$ for the Zn–Ni coatings obtained at the current densities: $\nabla - j = 20$ mA·cm^{-2}; $\blacktriangle$ – 30; $\blacksquare$ – 40; $\bigcirc$ – 50; $\square$ – 60 mA·cm^{-2}.
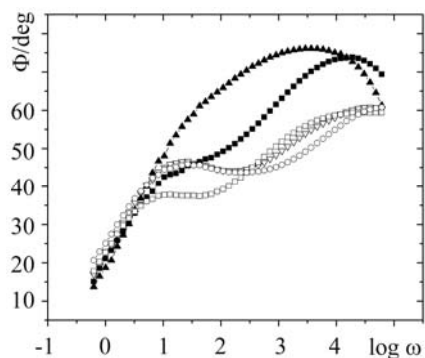

Fig. 5. Dependences of $\Phi = f(\log \omega)$ for the Zn–Ni coatings obtained at the current densities: $\nabla - j = 20$ mA·cm^{-2}; $\blacktriangle$ – 30; $\blacksquare$ – 40; $\bigcirc$ – 50; $\square$ – 60 mA·cm^{-2}.

Impedance measurements display a depressed semicircle on the complex plane plots. Examples of such plots for two coatings, which are characterized the extreme corrosion resistance (obtained at $j = 30$ and 50 mA·cm^{-2}) (Table 1) are presented in Fig. 3. Using the complex nonlinear least-squares (CNLS) fitting program, the real (Z') and imaginary (Z'') components of the impedance, could be analysed. The coating obtained at $j = 30$ mA·cm^{-2} exhibits the highest values of real and imaginary components. This means that this coating is most corrosion resistant in the 5% NaCl solution compared with the other obtained Zn–Ni coatings.

It has been found that the impedance of obtained coatings could be described by the two-CPE electrode model, which represents the solution resistance, R_s, in series with two parallel CPE – R_p elements (Fig. 6), explains the impedance behavior of the coating containing pear-shape pores (R_{p1}, R_{p2} [Ω·cm^2] are the polarization resistances, CPE$_1$, CPE$_2$ are the constant phase elements, where $Z_{CPE} = 1/[T(j\omega)^{\phi}]$ [11, 12]. The Nyquist plots, presented in Fig. 3, show a good agreement between the experimental points and approximations.
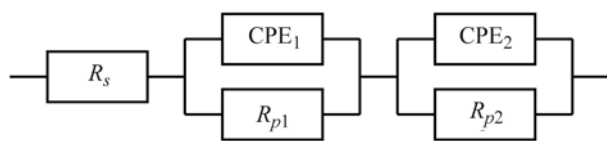
110

Fig. 6. Equivalent circuit scheme for the two-CPE electrode model.

As a result of approximation of the experimental data, the following parameters could be obtained: R_{p1}, T_1, ϕ_1, R_{p2}, T_2, ϕ_2 and R_s, where T_1, T_2 are the capacity parameters and ϕ_1, ϕ_2 are the CPE angles [10, 11]. Sum of $R_{p1} + R_{p2}$ gives a total value of polarization resistance, which is the highest for the Zn–Ni coating obtained at j = 30 mA·cm^{-2} (Table 2). The total values of R_p calculated by EIS method are approximately comparable with values of R_p obtained using potentiodynamic method and therefore it also could be a measure of corrosion resistance of coatings. The corrosion resistance of obtained coatings initially increases and then decreases with an increase in deposition current density. The maximum of corrosion resistance is observed for the coating deposited at j = 30 mA·cm^{-2}.

Table 2. Corrosion parameters of Zn–Ni coatings determined by EIS method depending on current density of deposition j

j, mA·cm^{-2}	R_{p1}, kΩ·cm^2	T_1	ϕ_1	R_{p2}, kΩ·cm^2	T_2	ϕ_2	R_s, Ω·cm^2
20	0.78	0.000092	0.53	5.98	0.000172	0.72	0.65
30	1.60	0.000014	0.60	35.88	0.000031	0.81	0.64
40	1.19	0.000024	0.66	15.60	0.000051	0.82	0.68
50	0.85	0.000076	0.59	7.56	0.000126	0.79	0.69
60	0.93	0.000058	0.55	7.94	0.000103	0.78	0.63

Values of logarithm of impedance module for the obtained coatings are comparable in the range of high frequency. These values are the highest in the range of low frequency for the Zn–Ni coating obtained at the current density of j = 30 mA·cm^{-2} (Fig. 4). Values of the phase angle for this coating, in the almost whole range of frequency are the highest and show a wide range of independence of a logarithm of angular frequency in comparison with the other coatings (Fig. 5). Moreover, $\Phi = f(\log\omega)$ dependences obtained for the coatings deposited at j = 20, 40, 50 and 60 mA·cm^{-2} are characterized by the presence of two time-constants but for the coating deposited at j = 30 mA·cm^{-2} only one time-constant is observed. Hence, it could be concluded that in the case of coating obtained at the current density of j = 30 mA·cm^{-2} only one phase corrodes and for the other coatings the corrosion process proceeds in two phases.

Based on these electrochemical investigations it was found that Zn–Ni coating obtained at j = 30 mA·cm^{-2} is more corrosion resistant in 5% NaCl solution than the other obtained Zn–Ni coatings.

Topography maps of deposited coatings were obtained using a Kelvin probe (Fig. 7).

It was stated that the coatings are characterized by a development area with an average height of unevenness from about 5 to 8 mm. Coatings deposited at the current density j = 30 and 40 mA·cm^{-2} are characterized by smaller development and greater uniformity of the surface compared with the coatings deposited at j = 20, 50 and 60 mA·cm^{-2}. Hence, the smallest number of corrosion centres can be expected for the Zn–Ni coating deposited at j = 30 and 40 mA·cm^{-2}.
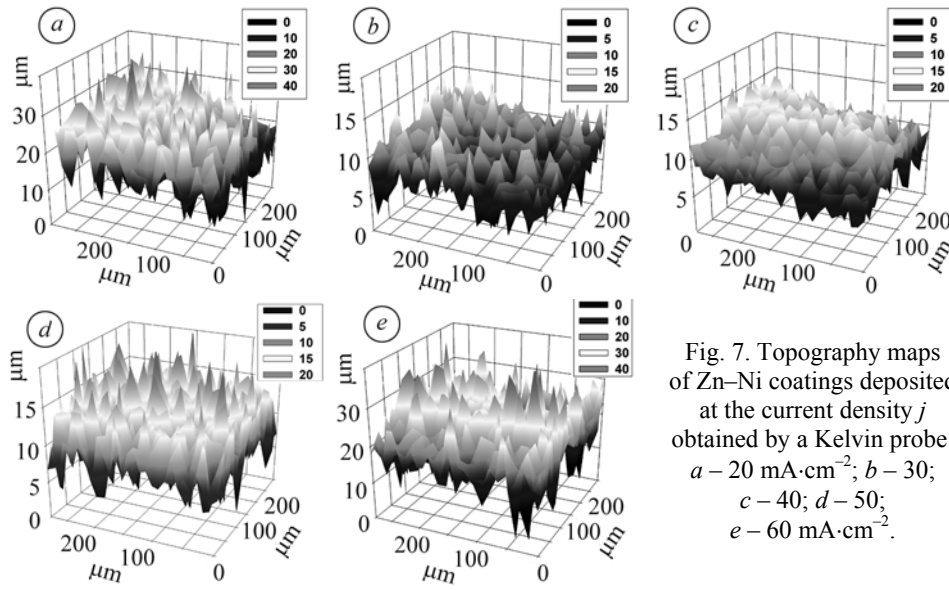
Fig. 7. Topography maps of Zn–Ni coatings deposited at the current density j obtained by a Kelvin probe: a – 20 mA·cm^{-2}; b – 30; c – 40; d – 50; e – 60 mA·cm^{-2}.

The SKP maps obtained for Zn–Ni coatings deposited at current density in the range of 20 to 60 mA·cm^{-2} show the differences in local potentials values (Fig. 8). It is observed that values of Kelvin potential difference measured at the surface of deposited coatings initially decrease and next increase with an increase in deposition current density. Recorded local potentials are in the range from $\Delta E = 0.3$ V to $\Delta E = 0.2$ V. It was found that the Zn–Ni coatings deposited at $j = 30$ and 40 mA·cm^{-2} are characterized by the smallest values of local potential and the most uniform their distribution on the surface (Fig. 8b, c). This means that these coatings are more resistant to local corrosion in comparison with coatings deposited at other current densities. This confirms the good corrosion resistance of these coatings, shown in studies of the total corrosion.
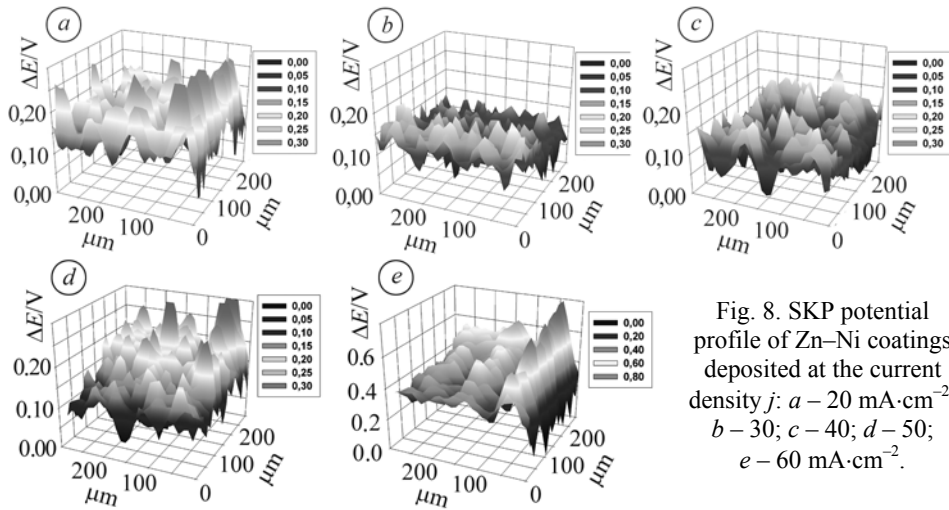

Fig. 8. SKP potential profile of Zn–Ni coatings deposited at the current density j: a – 20 mA·cm^{-2}; b – 30; c – 40; d – 50; e – 60 mA·cm^{-2}.

This correlates well with a small development of the surface of these coatings, which can lead to a smaller number of favored places of corrosive attack, compared to other Zn–Ni coatings.

112

Zn–Ni coatings obtained in the optimum range of current density were subjected to visual observation before and after the test in a salt chamber. It was found that the coatings are covered with little corrosion products. This demonstrates the good corrosion resistance of these coatings to the salt spray (Fig. 9).
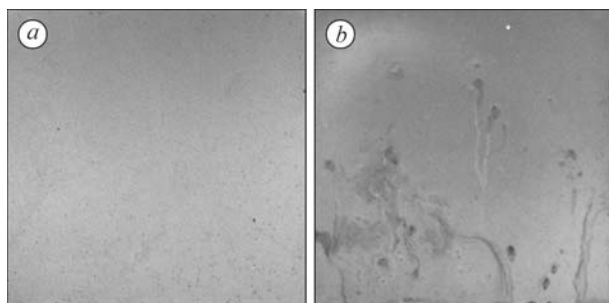

Fig. 9. Zn–Ni coating deposited at $j = 40$ mA·cm^{-2} before (*a*) and after (*b*) corrosion resistance investigations in a salt chamber.

CONCLUSIONS

On the basis of this research, the possibility of galvanostatic deposition of Zn–Ni coatings containing 14…18 at.% Ni is shown. It is stated, that surface morphology, chemical and phase composition of these coatings to a small degree depends on the current density of deposition. However, the current density of deposition determines the quantity of zinc which is co-deposited with nickel and is bound in the form of an intermetallic compound or a solid solution.

Small differences in chemical composition and the non-uniform distribution of Ni (Zn) and Ni$_2$Zn$_{11}$ phases on the surface of coatings, may cause local variations of Kelvin potential. As a consequence corrosion resistance of Zn–Ni coatings is varied depending on the current density. Coatings deposited at the current density $j = 30$ and 40 mA·cm^{-2} are characterized by the smallest values of local potential and the most uniform distribution on the surface.

On the ground of electrochemical investigations it is found that the Zn–Ni coatings obtained at the $j = 30$ and 40 mA·cm^{-2} are more corrosion resistant in 5% NaCl solution than the others Zn–Ni coatings. The lower value of corrosion current and also the higher value of polarization resistance results from above.

Moreover, it can be concluded that parameters calculated by EIS method can be a measure of corrosion resistance of coatings and results are confirmed by the potentiodynamic method.

РЕЗЮМЕ. Покриви на основі системи Zn–Ni гальваностатично осаджено за густини струму $j = 20…60$ mA·cm^{-2}. Досліджено вплив густини струму осадження на морфологію поверхні, хімічний та фазовий склад, а також корозійну тривкість. Для структурних випроб використано рентгенодифракційний метод (XRD). Морфологію поверхні та хімічний склад осадженого покриву вивчали на сканівному електронному мікроскопі JEOL JSM-6480, а корозійну тривкість – у 5%-му розчині NaCl, застосовуючи методи потенціодинамічної поляризації та електрохімічної імпедансної спектроскопії (EIS). Локальну корозійну тривкість визначено за допомогою методу сканівного зонда Кельвіна (SKP). Показано можливість осадження Zn–Ni із 14…18 at.% Ni. Встановлено, що морфологія поверхні, хімічний та фазовий склад цих покривів слабо залежать від густини струму осадження, яка, однак, визначає кількість цинку, що співосаджується з нікелем і зв'язаний у формі інтерметалічної сполуки або твердого розчину. Незначні відмінності у хімічному складі і нерівномірний розподіл фаз Zn(Ni) та Ni$_2$Zn$_{11}$ на поверхні покриву можуть спричинити відмінності у значеннях локального потенціалу Кельвіна. В результаті корозійна тривкість покривів на основі системи Zn–Ni змінюється залежно від густини струму осадження. Оптимальні значення густини струму, за яких корозійна тривкість покривів найвища, становлять $j = 30$ і 40 mA·cm^{-2}.

РЕЗЮМЕ. Покрытия на основе системы Zn–Ni гальваностатически осаждены при плотности тока $j = 20\ldots60$ mA·cm^{-2}. Исследовано влияние плотности тока осаждения на морфологию поверхности, химический и фазовый состав, а также коррозионную прочность. Для структурных экспериментов использован рентгенодифракционный метод (XRD). Морфологию поверхности и химический состав осажденного покрытия изучали на сканирующем электронном микроскопе JEOL JSM-6480, а коррозионную прочность – в 5%-ом растворе NaCl, применяя методы потенциодинамической поляризации и электрохимической импедансной спектроскопии (EIS). Локальная коррозионная прочность определена с помощью метода сканирующего зонда Кельвина (SKP). Показана возможность осаждения Zn–Ni с 14…18 at.% Ni. Выявлено, что морфология поверхности, химический и фазовый состав этих покрытий слабо зависят от плотности тока осаждения, которая, тем не менее, определяет количество цинка, осажденного вместе с никелем и связанного в форме интерметаллического соединения или твердого раствора. Незначительные отличия в химическом составе и неравномерное распределение фаз Zn(Ni) и Ni$_2$Zn$_{11}$ на поверхности покрытия могут обусловить отличия в значениях локального потенциала Кельвина. В результате коррозионная прочность покрытий на основе системы Zn–Ni изменяется в зависимости от плотности тока осаждения. Оптимальные значения плотности тока, при которых коррозионная прочность покрытий наиболее высокая, составляют $j = 30$ и 40 mA·cm^{-2}.

1. *Electroplating* of zinc–nickel binary alloys from acetate baths / S. S. Abd El Rehim, E. E. Fouad, S. M. Abd El Wahab, and H. H. Hassan // Electrochem. Acta. – 1996. – **41**, № 9. – P. 1413–1418.
2. *Fratesi R. and Roventi G.* Corrosion resistance of Zn–Ni alloy coatings in industrial production // Surf. Coat. Technol. – 1996. – **82**. – P. 158–164.
3. *Electrochemical* deposition and characterization of Zn–Co alloys and corrosion protection by electrodeposited epoxy coating on Zn–Co alloy / J. B. Bajat, V. B. Mišković-Stankovic, M. D. Maksimović et al. // Electrochem. Acta. – 2002. – **47**. – P. 4101–4112.
4. *Ganesan P., Kumaraguru S. P., and Popov B. N.* Development of compositionally modulated multiplayer Zn–Ni deposits as replacement for cadmium // Surf. Coat. Technol. – 2007. – **201**. – P. 7896–7904.
5. *Corrosion* behaviour of epoxy coatings electrodeposited on galvanized steel and steel modified by Zn–Ni alloys / J. B. Bajat, Z. Kačarević-Popović, V. B. Mišković-Stankowić, and M. D. Maksimowić // Prog. Org. Coat. – 2000. – **39**. – P. 127–135.
6. *Corrosion* behaviour of zinc-nickel coatings, electrodeposited on steel / M. Gavrila, J. P. Millet, H. Mazille et al. // Surf. Coat. Technol. – 2000. – **123**. – P. 164–172.
7. *Ganesan P., Kumaraguru S. P., and Popov B. N.* Development of compositionally modulated multiplayer Zn–Ni deposits as replacement for cadmium // Ibid. – 2007. – **201**. – P. 7896–7904.
8. *Stripping* of Zn–Ni alloys deposited in acetate-chloride electrolyte under potentiodynamic and galvanostatic conditions / A. Petrauskas, L. Grinceviciene, A. Cesuniene, and E. Matulionis // Ibid. – 2005. – **192**, № 2–3. – P. 299–304.
9. *Dependence* of coating characteristics on deposition potential for electrodeposited Zn–Ni alloys / F. Elkhatabi, M. Benballa, M. Sarret, and C. Muller // Electrochem. Acta. – 1999. – **44**, № 10. – P. 1645–1653.
10. *Soares M. E., Souza C. A., and Kuri C. S. E.* Corrosion resistance of a Zn–Ni electrodeposited alloy obtained with a controlled electrolyte flow and gelatin additive // Surf. Coat. Techn. – 2006. – **201**, № 6. – P. 2953–2959.
11. *Karimi-Shervedani R. and Lasia A.* Kinetics of hydrogen evolution reaction on nickel-zinc-phosphorous electrodes // J. Electrochem. Soc. – 1997. – **144**, № 8. – P. 2652–2657.
12. *Karimi-Shervedani R. and Lasia A.* Study of the hydrogen evolution reaction on Ni–Mo–P electrodes in alkaline solutions // Ibid. – 1998. – **145**, № 7. – P. 2219–2225.